Microsolvation and Protonation Effects on Geometric and Electronic Structures of Tryptophan and Tryptophan-Containing Dipeptides

Akimasa Fujihara, Naoki Noguchi, Yuji Yamada, Haruki Ishikawa, and Kiyokazu Fuke*

Department of Chemistry, Graduate School of Science, Kobe University, Rokkodai, Nada-ku, Kobe 657-8501, Japan

Received: March 18, 2009; Revised Manuscript Received: May 25, 2009

Photodissociation spectroscopy of solvated clusters of protonated tryptophan ($TrpH^+$) and dipeptides containing tryptophan (Val-$TrpH^+$, Ala-$TrpH^+$, and Gly-$TrpH^+$) has been carried out at low temperature to investigate the protonation and solvation effects on the electronic spectrum. For the protonated dipeptides, the S_1-S_0 transition exhibits a substantial red shift due to the stronger interaction between the NH_3^+ group and the indole π ring. The S_1-S_0 spectra of $TrpH^+(CH_3OH)_n$ clusters exhibit a drastic change with the number of methanol molecules. This behavior is interpreted in terms of the decrease in the interaction between the $\pi\pi^*$ and the repulsive $\pi\sigma^*$ states. Ala-$TrpH^+$ and Gly-$TrpH^+$ exhibit an extensive spectral change with addition of two methanol molecules. This change is ascribed to a conformational change, which is induced by the insertion of solvent molecule in between the NH_3^+ group and the indole π ring.

1. Introduction

Since the early 1980s, the experimental and theoretical studies of a variety of gas-phase clusters have been performed to reveal microscopic aspects of the condensed phase phenomena.[1−6] Although many efforts have been paid to explore the methods to study the physical and chemical properties of clusters, the experimental studies with well-defined or controlled temperature have been limited because of the difficulty in controlling the temperature of gas-phase clusters. To examine microscopic aspects of phase transition, structural fluctuation, and reactivity of clusters, it is necessary to perform spectroscopic measurements of gas-phase clusters at various temperatures. Gerlich and co-workers have developed a multipole radio frequency ion trap cooled by a refrigeration system and have studied ion−molecule reactions related to interstellar chemistry.[7,8] The collisional cooling in the trap is one of the most general methods for the temperature control of gas-phase ions. In the trap, the buffer gas filled in the entire region at a well-defined temperature and pressure thermalizes the trapped ions by multiple collisions as a thermal bath. We have been investigating microscopic solvation process in clusters using spectroscopic methods as a function of cluster size.[6,9−14] In order to conduct a spectroscopic study of gas-phase cluster ions as a function of temperature, we constructed a photodissociation spectrometer containing the temperature-controlled multipole ion trap and a spray ionization source and studied the structure and reactivity of cold protonated peptides.[15]

Primary and secondary structures of polypeptides are one of the important factors in the characterization of physical and chemical properties of biological molecules. At room temperature, a lot of conformers coexist, which correspond to local minima in the potential energy landscape, and conformational fluctuations play important roles in various functions of biological molecules. In recent years, a large number of spectroscopic studies in supersonic jet have succeeded in the conformational determination of neutral peptides in the gas phase.[16−19] The structural study in the solvent-free condition is considered to be important to extract an intrinsic property of biological molecules. Infrared multiphoton dissociation (IRMPD) spectroscopy of gas-phase protonated peptides has been performed extensively to gain structural information on the ions.[20−23] In such experiments, ions trapped in an ion cyclotron resonance cell or a Paul trap are irradiated with IR laser pulses for a few seconds until fragmentations occur resulting from the stepwise absorption of multiple photons. IRMPD spectra are obtained by monitoring fragment ions as a function of excitation energy. An important issue in the IRMPD experiments on trapped ions at room temperature is the conformational changes and isomerizations of the trapped ions during the stepwise absorption of IR photons over a few seconds. Since the vibrational energy absorbed is redistributed within a molecule on picosecond time scale,[24] IRMPD spectra may lack the spectral features specific to the low-lying energy conformers. In relation to this problem, Grégoire et al. performed ab initio Car−Parrinello molecular dynamics simulations of protonated peptides at 300 K.[23] With a comparison between the experimental IRMPD spectra and the predictions from the calculations, they showed that isomerization and intramolecular proton transfer occur spontaneously at 300 K. To avoid such an ambiguity, spectroscopic measurements of cold ions and their clusters are necessary. Rizzo and co-workers have performed infrared-ultraviolet (IR-UV) double-resonance spectroscopy of protonated amino acids and peptides in an ion trap cooled to 6 K.[25−27] The geometrical structures of the ions at low temperature have been revealed from comparison with density functional theory calculations.

Conformations of biological molecules are one of the important factors in determining their properties and are affected largely by solvation and/or temperature. In the previous study, we have measured UV photodissocation spectra of protonated dipeptides including tryptophan moiety at 20 K and higher temperatures. From these results, we discussed the interaction between the protonation site and π electron systems and the temperature effect on the relative distributions of several conformers.[15] We also examined the structures of solvated dipeptides using IR photodissociation spectroscopy.

Another interesting topic is the protonation effect on the electronic structure of biological molecules. Recently, the

* Corresponding author. E-mail: fuke@kobe-u.ac.jp. Phone and Fax: +81-78-803-5673.

10.1021/jp902451k CCC: $40.75
Published on Web 07/01/2009

electronic structure and relaxation dynamics of protonated tryptophan in the gas phase have been the subject of intensive studies.[28−31] Especially, the protonation effect on the electronic spectrum has been attracting considerable attention because that in solution has been studied extensively for the last decades.[32,33] The gas-phase studies predicted that the absorption of protonated tryptophan is in the same energy range as the S_1-S_0 transition of neutral tryptophan.[28,30,34] Weinkauf and co-workers reported the origin of $TrpH^+$ at 284.5 nm, which is only shifted by 2.3 nm (282 cm^{-1}) from the neutral Trp (286.8 nm).[28] Since the S_1-S_0 spectrum of $TrpH^+$ is so broad, it is considered to be difficult to make a further investigation into the protonation effect. In the previous work, we measured UV photodisociation spectra of protonated alanyltryptophan (Ala-$TrpH^+$) and tryptophanylglycine (Trp-$GlyH^+$) at several temperatures.[15] It is revealed that the electronic structure of the indole π electron system in Ala-$TrpH^+$ is strongly affected by the interaction with the NH_3^+ group, while the spectrum of Trp-$GlyH^+$ is very similar to that of $TrpH^+$ because of the weak interaction due to the geometrical structure restricting the close contact between the protonation site and the indole π ring.

In the present study, we have measured UV spectra of protonated valinyltryptophan (Val-$TrpH^+$) and glycyltryptophan (Gly-$TrpH^+$) to gain further insight into the protonation effect on the electronic spectrum. We have also measured UV spectra of protonated tryptophan ($TrpH^+$) and dipeptides including a tryptophan unit such as Ala-$TrpH^+$ and Gly-$TrpH^+$, as a function of solvent number and/or temperature. On the basis of these results as well as the theoretical calculations, we will discuss the effect of protonation and solvation on the geometric and electronic structures of biologically relevant molecules.

2. Experimental Section

Details of the experimental apparatus for the present photodissociation spectroscopy of temperature-controlled gas-phase biological cluster ions have been described previously.[15] The apparatus consists of five differentially evacuated chambers: a spray interface, an octopole ion guide, a quadrupole mass filter for mass selection of precursor ions, a temperature-variable multipole ion trap, and a quadrupole mass filter for mass analysis of fragment ions. Protonated tryptophan and dipeptides solvated with solvent molecules are generated by the spray ionization method and transferred to the gas phase through a metal capillary and a skimmer. The ions guided by the octopole are deflected 90° by an ion bender into the first quadrupole mass filter. The mass-selected ions are decelerated and refocused by a stack of electrostatic ion lenses into the temperature-variable multipole ion trap (10−350 K). The ions are stored and thermalized by multiple collisions with He buffer gas in the trap for ~80 ms and then irradiated with a photodissociation laser pulse. The product ions are extracted from the trap and analyzed by the second quadrupole mass filter. Photodissociation spectra are obtained by monitoring fragment ions as a function of excitation energy. UV laser pulses are generated by frequency doubling of a Nd:YAG (Continuum, NY61) pumped dye laser (Continuum, ND60) using a KDP crystal.

Geometry optimizations are carried out by a DFT calculation at the B3LYP/6-31++G(d,p) level using GAUSSIAN 03.[35] In the present study, we have performed optimizations for each species starting from many initial configurations according to the conformers in the reports for similar systems.[15,26,30,36] Geometries of the ions were optimized using the energy gradient technique at the B3LYP/6-31++G(d,p) level. Vibrational analyses were carried out at each optimized structure to confirm the minima on the potential energy surfaces. The zero-point vibrational correction (ZPC) was included in the calculated binding energies using scaled harmonic frequencies, in which the scale factor 0.956 was used.

3. Results and Discussion

3.1. Protonation Effect. To gain more insight into the protonation effect on the electronic spectrum of the indole π electron system as mentioned in Introduction, we have conducted the photodissociation spectroscopy of cold Val-$TrpH^+$ and Gly-$TrpH^+$, where the amino acids are bonded to the N-terminal of tryptophan as the sequence of Ala-$TrpH^+$. Previously, we measured the UV photodissociation spectrum of Trp-$GlyH^+$, where glycine is bonded to the C-terminal of tryptophan, in the energy region of the S_1-S_0 transition of the indole moiety.[15] The spectral feature is very similar to that of $TrpH^+$ over a wide temperature range from 20 to 300 K. With the aid of the quantum chemical calculations, it was found that the stable conformers of Trp-$GlyH^+$, where the glycine moiety is on the opposite side of the indole π ring, are similar to that of $TrpH^+$. In the conformers of $TrpH^+$ and Trp-$GlyH^+$, the distance between the NH_3^+ group and the indole π ring is substantially large because of the geometrical restriction by a $C_\alpha-C_\beta$ bond. Thus, the interaction between the two groups is too weak to affect the S_1 excited state of the indole moiety.

On the other hand, the amino groups of Val-$TrpH^+$ and Gly-$TrpH^+$ are able to form a close contact to the indole moiety as in the case of Ala-$TrpH^+$. Photodissociation spectra of Val-$TrpH^+$ and Gly-$TrpH^+$ at 20 K are shown in Figure 1. For comparison, the results on $TrpH^+$ and Ala-$TrpH^+$ are also displayed, which are cited from our previous paper.[15] As in the case of Ala-$TrpH^+$, the S_1-S_0 band origin of Val-$TrpH^+$ and Gly-$TrpH^+$ also exhibits a significant red shift by ~2000 cm^{-1} with respect to that of $TrpH^+$. If we look at the spectra more closely, we may see small difference in the absorption edges. From Gly-$TrpH^+$ to Val-$TrpH^+$, the absorption edge slightly shifts to the blue. Parts a and b of Figure 2 show the optimized structures of Val-$TrpH^+$ and Gly-$TrpH^+$, respectively. In the lowest-energy structures **Ia** for Val-$TrpH^+$ and **IIa** for Gly-$TrpH^+$, the protonation site is the amino group, and one of the H atoms of the NH_3^+ group points to the CO moiety of the amide group and another H atom binds to the π orbital of the indole moiety. These geometrical structures are similar to that of Ala-$TrpH^+$ shown as **VIa** in Figure 7, where the NH_3^+ group approaches the indole π ring. Therefore, the red shifts observed in the spectra of Val-$TrpH^+$ and Gly-$TrpH^+$ are ascribed to the stabilization of the excited state due to the strong interaction between the NH_3^+ group and the indole π ring resulting from the flexible geometrical structures of these dipeptides.

In the structural optimization, it is found that the protonation site of the most stable isomers is the amino group. However, we also find tautomers whose protonation site is the amide oxygen among relatively low-energy isomers. The structures of such tautomers are shown in Figure 2 as **Ib** and **IIb**. They are the tautomers of **Ia** and **IIa**, respectively. It is considered that these tautomers may be formed in the proton transfer reaction of the lowest-energy conformers such as **Ia** and **IIa**. The relative energies of the tautomers, **Ib** and **IIb,** with respect to the corresponding lowest-energy conformers are 4.26, 3.26, and 1.90 kcal/mol for Val-$TrpH^+$, Ala-$TrpH^+$, and Gly-$TrpH^+$, respectively. These tautomers were not identified in the present experiments as mentioned in section 3.2.2.

3.2. Solvation Effect. ***3.2.1. $TrpH^+(CH_3OH)_n$.*** Figure 3 shows photodissociation spectra of $TrpH^+(CH_3OH)_n$ at 20 K in

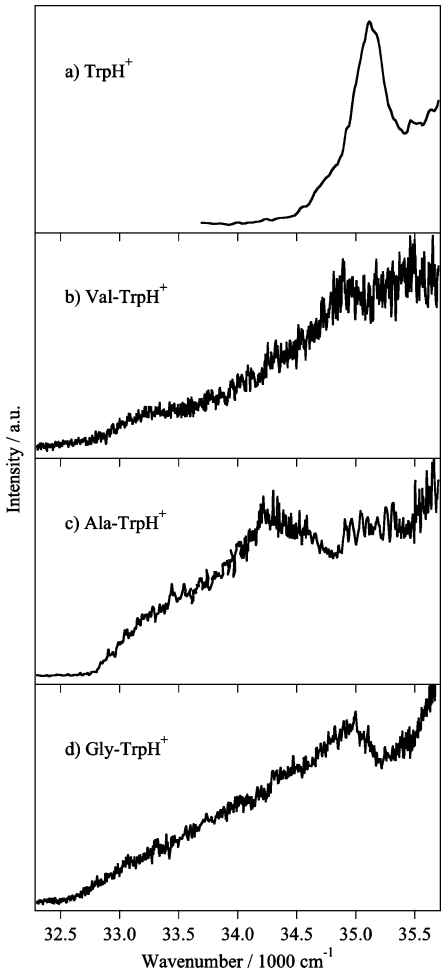

Figure 1. Photodissociation spectra of (a) $TrpH^+$, (b) Val-$TrpH^+$, (c) Ala-$TrpH^+$, and (d) Gly-$TrpH^+$ at 20 K.

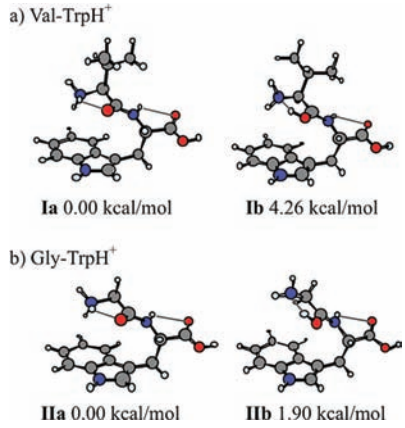

Figure 2. Selected sets of optimized structures of (a) Val-$TrpH^+$ and (b) Gly-$TrpH^+$ at the B3LYP/6-31++G(d,p) level. Relative binding energies with ZPC are given under each structure. The protonation sites are the amino nitrogen, **Ia** and **IIa**, and the amide oxygen, **Ib** and **IIb**, respectively.

the energy region of the lowest $\pi\pi^*$ transition of the indole moiety. The S_1-S_0 band origin of $TrpH^+$ is observed at 35 100 cm^{-1}. The broad bandwidth of 235 cm^{-1} is attributed to a short lifetime of the excited-state $TrpH^+$, which is due to the mixing of the $\pi\pi^*$ state with the dissociative $\pi\sigma^*$ state.[29−31] With the addition of one methanol molecule, the band becomes slightly narrower by 65 cm^{-1}. The addition of another methanol molecule makes a drastic change in the spectrum as shown in

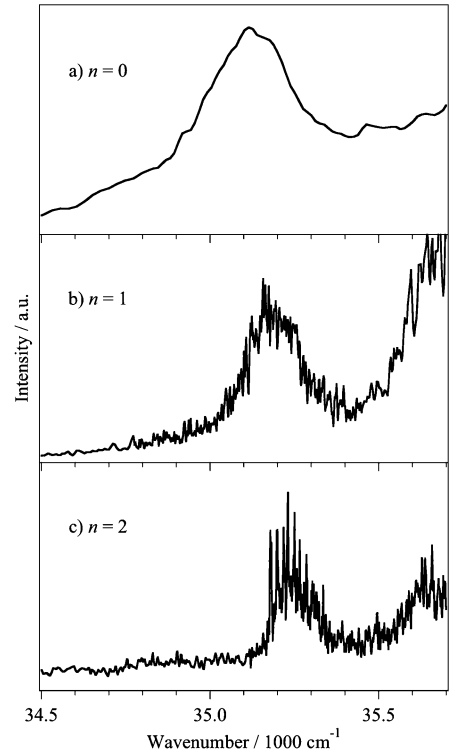

Figure 3. Photodissociation spectra of $TrpH^+(CH_3OH)_n$ at 20 K.

Figure 3c. $TrpH^+(CH_3OH)_2$ exhibits a vibrationally resolved electronic spectrum, implying that the addition of two methanol molecules significantly lengthens the excited-state lifetime. Similar change in the electronic spectrum by addition of solvent molecules is reported by Mercier et al. for $TrpH^+(H_2O)_n$.[36] Their simulations of the excited-state dynamics of $TrpH^+(H_2O)_2$ suggest that the solvation of the NH_3^+ group by two water molecules, where all of the H atoms in the NH_3^+ group are hydrogen-bonded, destabilizes the dissociative $\pi\sigma^*$ state, and the mixing of the $\pi\pi^*$ state with the $\pi\sigma^*$ state is weakened. As a result, the excited-state lifetime becomes longer, and $TrpH^+(H_2O)_2$ exhibits well-resolved vibronic bands in the S_1-S_0 spectrum. The present results on $TrpH^+(CH_3OH)_2$ may be in a similar situation.

To gain further insight into the solvation effect on the electronic spectrum, possible conformations of $TrpH^+(CH_3OH)_2$ are calculated. Optimized structures of $TrpH^+(CH_3OH)_2$ and the stable structure of $TrpH^+$ and $TrpH^+(CH_3OH)$ observed in our previous experiments[15] are shown in Figure 4. The conformer **Va** of $TrpH^+(CH_3OH)_2$ obtained in our calculations has a structure similar to that proposed by Mercier et al. for $TrpH^+(H_2O)_2$.[36] In the conformer **Va**, the NH_3^+ group is bound to two methanol molecules and the CO moiety of the carboxyl group; that is, all of the three ammonium N−H bonds are involved in hydrogen bonds. We can identify three low-frequency progressions of the 20 cm^{-1} interval in the spectrum as shown in Figure 5a. In the case of $TrpH^+(H_2O)_2$, similar progressions of the 27 cm^{-1} interval have been observed.[36] Based on our calculations, this low-frequency mode can be assigned as a torsional motion around the $C_\alpha-C_\beta$ bond of $TrpH^+$. Although the present calculations are for the electronic ground state, shifts in the vibrational frequency when we change the solvents from H_2O to CH_3OH are quite reasonable. In the case of $TrpH^+(CH_3OH)_2$, the conformer **Va** lies 3.14 kcal/mol higher in energy than the conformer **Vc** where one of methanol molecules is bonded to the carboxyl group. In the lowest-energy

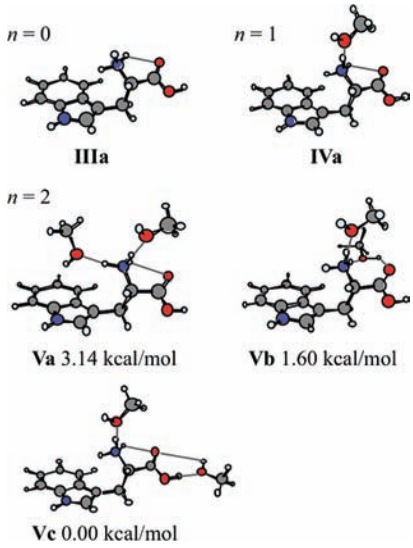

Figure 4. Selected sets of optimized structures of $TrpH^+(CH_3OH)_n$ at the B3LYP/6-31++G(d,p) level. Relative binding energies with ZPC of $TrpH^+(CH_3OH)_2$ are given under each structure.

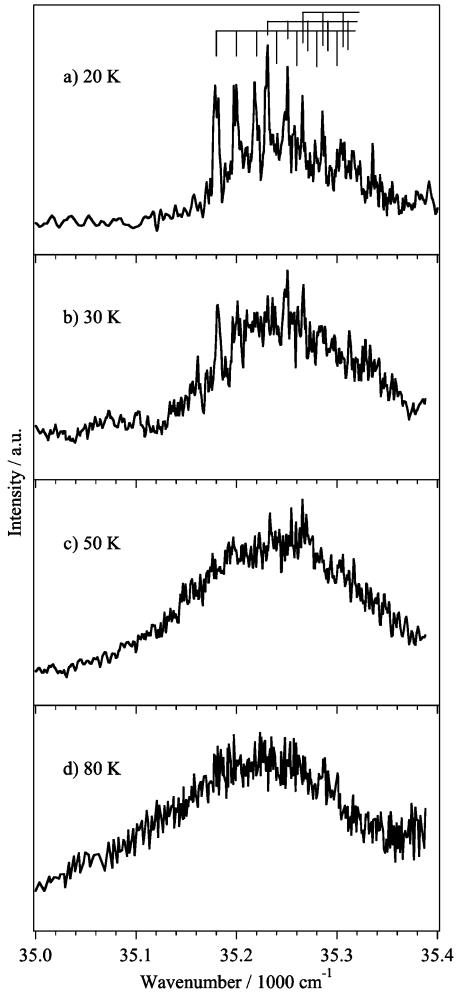

Figure 5. Photodissociation spectra of $TrpH^+(CH_3OH)_2$ at 20−80 K. Low-frequency progressions of the 20 cm^{-1} interval are indicated in trace a.

conformer **Vc**, the solvation structure of the NH_3^+ group is similar to that of $TrpH^+(CH_3OH)$ such as **IVa** which exhibits an unresolved broad band as shown in Figure 3b. However, we assigned the spectral carriers of the vibrationally resolved bands to be **Va** and/or the conformers having a structure similar to **Va**, based on the fact of the drastic change in the excited-state lifetime as in the case of $TrpH^+(H_2O)_2$ reported by Mercier et al.[36] This conclusion is consisted with the above-mentioned assignment of the low-frequency progressions.

To examine temperature effects on solvated $TrpH^+$, photodissociation spectra of $TrpH^+(CH_3OH)_2$ have been measured at several temperatures. Figure 5 shows the photodissociation spectra of $TrpH^+(CH_3OH)_2$ at 20−80 K. The spectrum of $TrpH^+(CH_3OH)_2$ in the vicinity of the S_1-S_0 band origin at 20 K is expanded and shown in Figure 5a. In this spectrum, a broad background signal around 35 230 cm^{-1} appears on the foot of the vibrationally resolved bands. Upon raising the temperature from 20 to 30 K as shown in Figure 5b, a peak appears at 35 160 cm^{-1} in the spectrum at 30 K, which can be assigned as a hot band of the low-frequency torsional mode. In the spectra measured at higher than 50 K, sharp bands disappear and the only broad band around 35 230 cm^{-1} is observed. It is considered that the spectral changes with a rise in temperature are mostly ascribed to appearing of hot bands assigned to the low-frequency vibrational modes. We would also expect to see the conformational change at higher temperature as in the case of Ala-$TrpH^+$ mentioned later. However, the spectral shift by a structural change may be too small to distinguish the spectral changes. To examine detailed temperature effects on the structure of $TrpH^+(CH_3OH)_2$, it is necessary to perform infrared spectroscopy.

3.2.2. Ala-TrpH$^+$(CH$_3$OH)$_n$. In our previous study, it was found that the S_1-S_0 transition of Ala-$TrpH^+$ is red shifted by ~2000 cm^{-1} with respect to that of $TrpH^+$.[15] This significant change is attributed to the strong interaction between the NH_3^+ group and the indole π ring. In the case of Ala-$TrpH^+$, the elongation of the side chain enables a close contact between these two groups. In addition, it was found that the relative intensity of a conformer, which exhibits the S_1-S_0 transition very close to that of $TrpH^+$, increases in the spectrum when the temperature of the ions is raised to 80 K.[15] The result indicates the increase of the distribution of a conformer, which has a structure with longer distance between the protonation site and the indole π ring and suggests the occurrence of a thermally induced conformational change. We would also expect that the interaction between these groups may change by a stepwise solvation and that this effect may be observed as a change in the electronic spectrum. In order to gain more information on the relation between the solvation and conformational structures, we have measured the photodissociation spectra of cold Ala-$TrpH^+(CH_3OH)_n$.

Figure 6b shows the photodissociation spectrum of Ala-$TrpH^+(CH_3OH)_2$ at 20 K. The spectrum of Ala-$TrpH^+$ is also shown for comparison. In the case of Ala-$TrpH^+(CH_3OH)_2$, three bands are observed at around 34 950, 34 200, and 33 600 cm^{-1}. In addition to these bands, a new band appears at 32 900 cm^{-1}. Among these bands, the band at 34 950 cm^{-1} is the strongest and much enhanced compared with the bare Ala-$TrpH^+$. The peak position of this band is very close to those of the $TrpH^+$ and the conformer of Ala-$TrpH^+$ observed in the spectrum at 80 K. In order to assign these bands, we calculated the structure of Ala-$TrpH^+(CH_3OH)_2$. Optimized structures of the low-energy conformers of Ala-$TrpH^+(CH_3OH)_2$ are shown as **VIIa**−**VIId** in Figure 7. The most stable conformer of Ala-$TrpH^+$ calculated in our previous study is also shown as **VIa** in Figure 7. In the lowest energy conformer **VIIa**, two methanol molecules are directly hydrogen bonded to the NH bond of the NH_3^+ group. This structure is similar to those of the

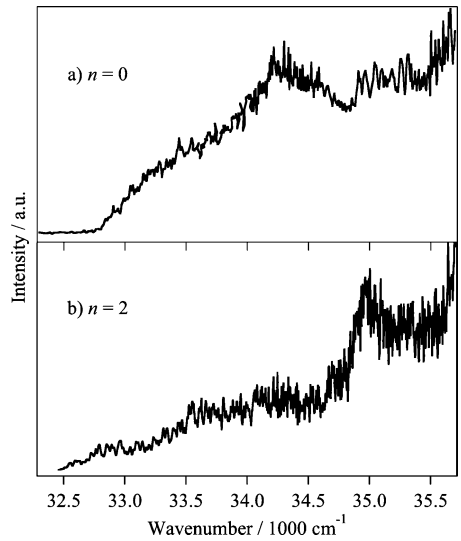

Figure 6. Photodissociation spectra of (a) Ala-TrpH$^+$ and (b) Ala-TrpH$^+$(CH$_3$OH)$_2$ at 20 K.

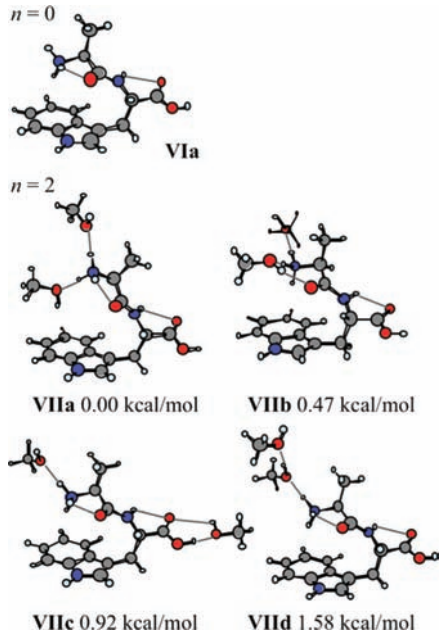

Figure 7. Selected sets of optimized structures of Ala-TrpH$^+$ and Ala-TrpH$^+$(CH$_3$OH)$_2$ at the B3LYP/6-31++G(d,p) level. Relative binding energies with ZPC of Ala-TrpH$^+$(CH$_3$OH)$_2$ are given under each structure.

TrpH$^+$(H$_2$O)$_2$ and TrpH$^+$(CH$_3$OH)$_2$. In the case of Ala-TrpH$^+$(CH$_3$OH)$_2$, one of the methanol molecules is inserted between the NH_3^+ group and the indole π ring. This methanol molecule acts as a proton acceptor for the NH_3^+ group whereas a proton donor for the indole π electron system. As a result of the insertion of the solvent molecule, two groups come apart and the spectrum shifts close to that of TrpH$^+$. Therefore, the strongest band at 34 950 cm^{-1} is reasonably attributed to the conformer **VIIa**. It is worth noticing that the 34 950 cm^{-1} band is also expected to exhibit a vibrationally resolved spectral feature, because **VIIa** has a similar structure to that of TrpH$^+$(CH$_3$OH)$_2$ as mentioned previously. With this structure, the aforementioned $\pi\sigma^*$ state, which is a Rydberg-type and has the repulsive nature, is destabilized by the interaction with solvents, and as a result, the lifetime of the first excited state is elongated as in the case of TrpH$^+$(CH$_3$OH)$_2$. However, the

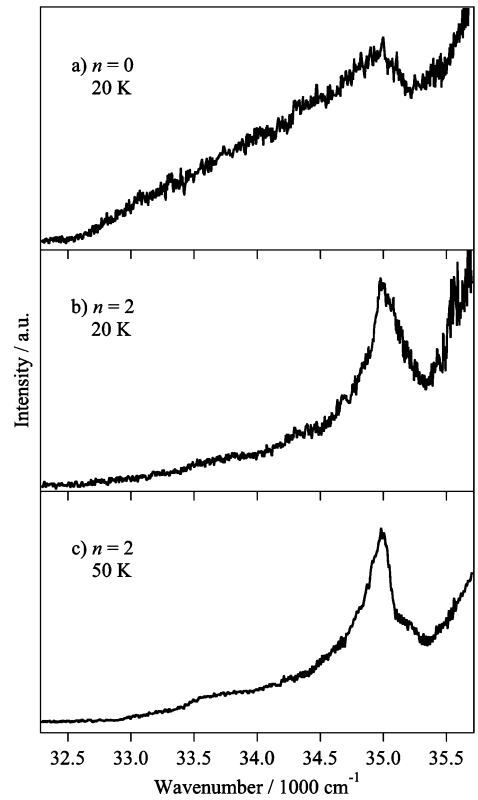

Figure 8. Photodissociation spectra of Gly-TrpH$^+$ at 20 K and Gly-TrpH$^+$(CH$_3$OH)$_2$ at 20 and 50 K.

34 950 cm^{-1} band of Ala-TrpH$^+$(CH$_3$OH)$_2$ exhibits the broad feature probably because of the existence of the other conformers, which have the structure close to **VIIa**.

On the other hand, for the other conformers such as **VIIb**, **VIIc**, and **VIId**, the distance between two groups is similar to that of the bare Ala-TrpH$^+$. In these structures, two methanol molecules bound to the surface of the closed-form conformer such as **VIIa**, and its solvation effect on the electronic spectrum is expected to be relatively weaker. These arguments suggest that the above conformers are the candidates of the carrier of the bands at around 34 200, 33 600, and 32 900 cm^{-1}. Therefore, these results clearly indicate that the conformational change is induced by solvation as well as thermally.

3.2.3. Gly-TrpH$^+$(CH$_3$OH)$_n$. We have also conducted the UV spectroscopy of solvated Gly-TrpH$^+$ at several temperatures to examine the solvation and temperature effects on the conformation of dipeptide. A photodissociation spectrum of Gly-TrpH$^+$(CH$_3$OH)$_2$ at 20 K is shown in Figure 8b. The feature of the solvation effect on the spectrum is similar to that of Ala-TrpH$^+$. With the solvation of two methanol molecules to the Gly-TrpH$^+$, the relative intensity of the broad band from 32 500 cm^{-1} to 34 500 cm^{-1} decreases drastically. On the contrary, the broad structureless band appears strongly at 34 980 cm^{-1}, which is located very close to the S_1-S_0 band origin of TrpH$^+$. Selected sets of optimized structures of Gly-TrpH$^+$(CH$_3$OH)$_2$ are shown as **VIIIa**, **VIIIb**, and **VIIIc** in Figure 9. In the lowest-energy conformer **VIIIa**, two methanol molecules are directly bound to the NH_3^+ group, and one of the methanol molecules is inserted between the NH_3^+ group and the indole π ring as in the case of Ala-TrpH$^+$(CH$_3$OH)$_2$ shown as **VIIa** in Figure 7. With this conformation, the interaction between the NH_3^+ group and the indole π ring becomes weaker than that of the bare Gly-TrpH$^+$. As a result, the S_1-S_0 transition energy of the conformer **VIIIa** is expected to be similar to those of TrpH$^+$

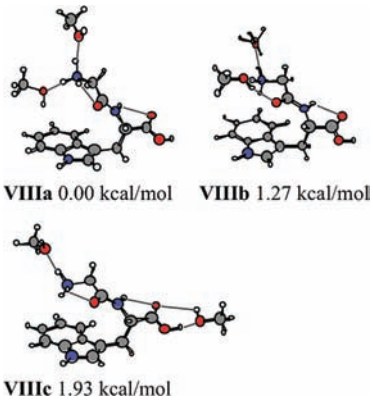

Figure 9. Selected sets of optimized structures of Gly-TrpH$^+$(CH$_3$OH)$_2$ at the B3LYP/6-31++G(d,p) level. Relative binding energies with ZPC are given under each structure.

and Trp-GlyH$^+$. Therefore, the band at 34 980 cm^{-1} is assigned to the S_1-S_0 transition of the conformer such as **VIIIa**. On the other hand, the weak bands appearing in the lower-energy region may be assigned to the S_1-S_0 transitions of the other conformers such as **VIIIb** and **VIIIc**, where Gly-TrpH$^+$ holds the closed-form and two methanol molecules bound to its surface as in the case of Ala-TrpH$^+$(CH$_3$OH)$_2$ discussed in section 3.2.2.

Figure 8c shows the UV spectrum of Gly-TrpH$^+$(CH$_3$OH)$_2$ at 50 K. The spectrum is similar to that measured at 20 K. This means that the lowest-energy conformer, where one methanol molecule is inserted between the NH_3^+ group and the indole π ring, is still dominant within the present temperature range. There are several minor changes in the spectrum at 50 K compared with that at 20 K. However, it is difficult to discuss such differences based on the information available at the present stage.

4. Conclusions

The photodissociation spectroscopy of solvated TrpH$^+$ and protonated dipeptides involving tryptophan has been carried out at well-defined temperatures to gain microscopic aspects for the protonation and solvation effects on the conformational change of biological molecules. We have observed the large protonation effect on the electronic spectra of Val-TrpH$^+$ and Gly-TrpH$^+$ in contrast to the case of TrpH$^+$, which exhibits no appreciable change in spectral shift. The large spectral change is ascribed to the close contact between the NH_3^+ group and the indole π ring caused by the flexible structure, which allows much stronger interaction between the two groups.

In the case of TrpH$^+$, the S_1-S_0 spectrum exhibits a drastic change with increasing the number of methanol molecules. This behavior is interpreted in terms of the decrease in the interaction between the $\pi\pi^*$ and repulsive $\pi\sigma^*$ states, which is induced by the solvation. For the Ala-TrpH$^+$ and Gly-TrpH$^+$ systems, we have observed the large spectral change in the lowest-energy transitions by solvation. These results are ascribed to the change in the relative abundance of conformers by solvation from the comparison with the calculated structures. Calculations of the optimized structures suggest that a methanol molecule is inserted between the NH_3^+ group and the indole π ring and thus lengthens the distance between these groups. The photodissociation spectra clearly show the predominance of this conformation and the solvent-induced conformational change.

Acknowledgment. This work is partially supported by the Grant-in-Aid for Scientific Research (Grant 18350009) and by the Grant-in-Aid for Scientific Research in Priority Areas (Grant 19056004) from the Ministry of Education, Culture, Sports, Science, and Technology (MEXT) of Japan, and also by a research grant from the Japan Science and Technology Agency.

References and Notes

(1) Castleman, A. W., Jr.; Bowen, K. H., Jr. *J. Phys. Chem.* **1996**, *100*, 12911.
(2) Lisy, J. M. *J. Chem. Phys.* **2006**, *125*, 132302.
(3) Verlet, J. R. R.; Bragg, A. E.; Kammrath, A.; Cheshnovsky, O.; Neumark, D. M. *Science* **2005**, *307*, 93.
(4) Stanford, T.; Andrews, D.; Rathbone, J.; Taylor, M.; Muntean, F.; Thompson, M.; McCoy, A. B.; Parson, R.; Lineberger, W. C. *Faraday Discuss.* **2004**, *127*, 383.
(5) Zewier, T. S. *Annu. Rev. Phys. Chem.* **1996**, *47*, 205.
(6) Fuke, K. *Trends Phys. Chem.* **2004**, *10*, 26.
(7) Gerlich, D. *Phys. Scr.* **1995**, *T59*, 256.
(8) Gerlich, D.; Horning, S. *Chem. Rev.* **1992**, *92*, 1509.
(9) Fuke, K.; Kaya, K. *Chem. Phys. Lett.* **1983**, *94*, 97.
(10) Misaizu, F.; Sanekata, M.; Fuke, K.; Iwata, S. *J. Chem. Phys.* **1994**, *100*, 1161.
(11) Okai, N.; Yoshida, S.; Aranishi, K.; Takahata, A.; Fuke, K. *Phys. Chem. Chem. Phys.* **2005**, *7*, 921.
(12) Takasu, R.; Taguchi, T.; Hashimoto, K.; Fuke, K. *Chem. Phys. Lett.* **1998**, *290*, 481.
(13) Fujihara, A.; Miyata, C.; Maekawa, A.; Fuke, K.; Daigoku, K.; Murata, N.; Hashimoto, K. *J. Phys. Chem. A* **2007**, *111*, 7364.
(14) Fuke, K.; Takasu, R. *Bull. Chem. Soc. Jpn.* **1995**, *68*, 3309.
(15) Fujihara, A.; Matsumoto, H.; Shibata, Y.; Ishikawa, H.; Fuke, K. *J. Phys. Chem. A* **2008**, *112*, 1457.
(16) Weinkauf, R.; Schermann, J.-P.; de Vries, M. S.; Kleinermanns, K. *Eur. Phys. J. D* **2002**, *20*, 309.
(17) Unterberg, C.; Gerlach, A.; Schrader, T.; Gerhards, M. *J. Chem. Phys.* **2003**, *118*, 8296.
(18) Chin, W.; Compagnon, I.; Dognon, J.-P.; Canuel, C.; Piuzzi, F.; Dimicoli, I.; von Helden, G.; Meijer, G.; Mons, M. *J. Am. Chem. Soc.* **2005**, *127*, 1388.
(19) Hünig, I.; Kleinermanns, K. *Phys. Chem. Chem. Phys.* **2004**, *6*, 2650.
(20) Oh, H.-B.; Lin, C.; Hwang, H. Y.; Zhai, H.; Breuker, K.; Zabrouskov, V.; Carpenter, B. K.; McLafferty, F. M. *J. Am. Chem. Soc.* **2005**, *127*, 4076.
(21) Fukui, K.; Takada, Y.; Sumiyoshi, T.; Imai, T.; Takahashi, K. *J. Phys. Chem. B* **2006**, *110*, 16111.
(22) Polfer, N. C.; Oomens, J.; Suhai, S.; Paizs, B. *J. Am. Chem. Soc.* **2007**, *129*, 5887.
(23) Grégoire, G.; Gaigeot, M. P.; Marinica, D. C.; Lemaire, J.; Schermann, J. P.; Desfrançois, C. *Phys. Chem. Chem. Phys.* **2007**, *9*, 3082.
(24) Yamada, Y.; Katsumoto, Y.; Ebata, T. *Phys. Chem. Chem. Phys.* **2007**, *9*, 1170.
(25) Stearns, J. A.; Mercier, S. R.; Seaiby, C.; Guidi, M.; Boyarkin, O. V.; Rizzo, T. R. *J. Am. Chem. Soc.* **2007**, *129*, 11814.
(26) Stearns, J. A.; Guidi, M.; Boyarkin, O. V.; Rizzo, T. R. *J. Chem. Phys.* **2007**, *127*, 154322.
(27) Stearns, J. A.; Seaiby, C.; Boyarkin, O. V.; Rizzo, T. R. *Phys. Chem. Chem. Phys.* **2009**, *11*, 125.
(28) Nolting, D.; Marian, C.; Weinkauf, R. *Phys. Chem. Chem. Phys.* **2004**, *6*, 2633.
(29) Kang, H.; Jouvet, C.; Lardeux, C.-D.; Martrenchard, S.; Grégoire, G.; Desfrançois, C.; Schermann, J.-P.; Barat, M.; Fayeton, J. A. *Phys. Chem. Chem. Phys.* **2005**, *7*, 394.
(30) Grégoire, G.; Jouvet, C.; Dedonder, C.; Sobolewski, A. L. *Chem. Phys.* **2006**, *324*, 398.
(31) Boyarkin, O. V.; Mercier, S. R.; Kamariotis, A.; Rizzo, T. R. *J. Am. Chem. Soc.* **2006**, *128*, 2816.
(32) Robbins, R. J.; Fleming, G. R.; Beddard, G. S.; Robinson, G. W.; Thistlethwaite, P. J.; Woolfe, G. J. *J. Am. Chem. Soc.* **1980**, *102*, 6271.
(33) Callis, P. R.; Liu, T. *J. Phys. Chem. B* **2004**, *108*, 4248.
(34) Rizzo, T. R.; Park, Y. D.; Peteanu, L. A.; Levy, D. H. *J. Chem. Phys.* **1986**, *84*, 2534.
(35) Frisch, M. J.; Trucks, G. W.; Schlegel, H. B.; Scuseria, G. E.; Robb, M. A.; Cheeseman, J. R.; Montgomery, J. A., Jr.; Vreven, T.; Kudin, K. N.; Burant, J. C.; Millam, J. M.; Iyengar, S. S.; Tomasi, J.; Barone, V.; Mennucci, B.; Cossi, M.; Scalmani, G.; Rega, N.; Petersson, G. A.; Nakatsuji, H.; Hada, M.; Ehara, M.; Toyota, K.; Fukuda, R.; Hasegawa, J.; Ishida, M.; Nakajima, T.; Honda, Y.; Kitao, O.; Nakai, H.; Klene, M.; Li, X.; Knox, J. E.; Hratchian, H. P.; Cross, J. B.; Bakken, V.; Adamo, C.; Jaramillo, J.; Gomperts, R.; Stratmann, R. E.; Yazyev, O.; Austin, A. J.;

Cammi, R.; Pomelli, C.; Ochterski, J. W.; Ayala, P. Y.; Morokuma, K.; Voth, G. A.; Salvador, P.; Dannenberg, J. J.; Zakrzewski, V. G.; Dapprich, S.; Daniels, A. D.; Strain, M. C.; Farkas, O.; Malick, D. K.; Rabuck, A. D.; Raghavachari, K.; Foresman, J. B.; Ortiz, J. V.; Cui, Q.; Baboul, A. G.; Clifford, S.; Cioslowski, J.; Stefanov, B. B.; Liu, G.; Liashenko, A.; Piskorz, P.; Komaromi, I.; Martin, R. L.; Fox, D. J.; Keith, T.; Al-Laham, M. A.; Peng, C. Y.; Nanayakkara, A.; Challacombe, M.; Gill, P. M. W.; Johnson, B.; Chen, W.; Wong, M. W.; Gonzalez, C.; Pople, J. A. *Gaussian 03*, revision C.02; Gaussian, Inc.: Wallingford, CT, 2004.

(36) Mercier, S. R.; Boyarkin, O. V.; Kamariotis, A.; Guglielmi, M.; Tavernelli, I.; Cascella, M.; Rothlisberger, U.; Rizzo, T. R. *J. Am. Chem. Soc.* **2006**, *128*, 16938.

JP902451K